

## Paper A

# Simulation for Advanced Control of a Paper Machine: Model Complexity and Model Reduction

Hauge, T.A. and Lie, B. (2000). *Simulation for Advanced Control of a Paper Machine: Model Complexity and Model Reduction*, in proceedings of the 41st SIMS simulation Conference, September 18-19, 2000, Technical University of Denmark, Kgs. Lyngby, Denmark, p 135-154.

A few corrections are made to the original paper.

# Simulation for Advanced Control of a Paper Machine: Model Complexity and Model Reduction

T. A. Hauge and B. Lie  
Telemark University College  
Kjolnes Ring 56  
3914 Porsgrunn  
Norway

## Abstract

A 528 order mechanistic model of a paper machine is implemented in Matlab. The model has been developed for advanced control of three key quality variables, and it is desirable to reduce the size and complexity of the full scale model. It is shown how the full scale model can be reduced by both system identification techniques and by utilizing our physical knowledge about the process. The prediction abilities of the various reduced order models are compared with the output from the 528 order model, highlighting some distinct features of the various models.

**Keywords:** Paper machine, dynamic model, model complexity, model reduction, system identification

## 1 Introduction

The world's second largest manufacturer of uncoated magazine paper (SC) is Norske Skog Saugbrugs, at Halden, Norway (Norske Skog 2000). Magazine paper is characterized by its glossy appearance due to the high content of filler (usually clay). Typically 30% (weight %) of the paper consists of filler, 65% of fibers and 5% of water. The filler is added for improving certain properties of the paper, such as brightness and smoothness, and also often to reduce the production costs. The Saugbrugs mill incorporates three paper machines (PM), in which PM6 is the largest and most modern one (built in the 1990's). A paper machine is in general a multivariable non-linear complex mixture of mechanical and chemical processes. A model of such a machine must capture the essential behavior with respect to a set of chosen variables. Typically the term "essential" will have different meaning to scientists working in different areas. A model for control should have input-output properties reasonably close to the input-output properties of the true system, while still be simple enough for implementation and use in real-time applications. There are basically two different approaches to modeling for control: i) Mechanistic modeling, in which physics,

material balances, etc. form the basis of the model, and ii) Empirical modeling, in which collected input-output data are used to fit a non-physical model structure to the data. The two approaches have some distinct features which will be discussed later.

At Norske Skog Saugbrugs, a project has been initiated to implement advanced model based control for some key paper quality variables at PM6. A mechanistic model of PM6, with three selected output variables and three selected input variables, has been developed and implemented in MATLAB. This work is thoroughly described in (Hauge & Lie 2000). The model, which is a non-linear state-space model, is quite large and complex, and perhaps not a good candidate for model based control. Input-output data are collected from the process and these indicate that first- or second-order submodels with time delays may be sufficient to describe the process behavior (at a given operating condition) (Slora 1999). Thus, the problem is to reduce the complexity of the model so that it is more suitable for advanced control purposes.

There are many benefits of simplified models, e.g. less computational time, and easier analysis, interpretation and controller design. However, the accuracy of a simplified model will in general decrease. A lot of work has been done in the area of model reduction - see e.g. (Öhman 1998), (Andersson 1997) and (Diwekar 1994). These references focus on e.g. model reduction within specified error bounds or along known trajectories. In this paper we approach the simplification problem by i) system identification methods - i.e. we identify empirical “low order” models by various well established methods, and ii) physical knowledge - i.e. we utilize our physical knowledge about the process to reduce the model. Finally, we compare the various reduced models and test their prediction abilities at different operating conditions.

The full scale mechanistic model will be used as a reference for comparison with models of reduced complexity. The comparison will be done by simulation studies, and we will investigate how the reduced complexity influence on the input-output behavior of the system. Thus, we only consider the  $\hat{y}_{k|0}$  predictor in this paper, i.e. the predicted output  $\hat{y}$  at time  $k$ , given  $y$  at time 0. Another well known predictor is the one-step-ahead predictor  $\hat{y}_{k+1|k}$ .

## 2 The Process

A simplified overview of PM6 is given in Figure 1. Cellulose, TMP (thermomechanical pulp) and broke (repulped fibers and filler from sheet breaks and edge trimmings) are blended in the mixing chest. The stock is fed to the machine chest with a controlled total consistency<sup>1</sup>. Between the mixing and machine chests, filler is added at a constant rate. The filler is usually clay, but occasionally another kind of filler is added when high whiteness is required. The flow to the machine chest is large in order to keep the level of the machine chest constant, and an overflow is returned to the mixing chest. The total consistency in the mixing and machine chests are typically around

---

<sup>1</sup>The total consistency is the weight of solids (i.e. filler, fiber and fines) divided by the total weight of solids and water.

3 to 4%, which is considerably higher than consistencies later on in the process, and thus the stock from the machine chest is denoted as the “thick stock”.

The thick stock enters the “short circulation” in the white water tank. Here, the thick stock is diluted to 1-1.5% total consistency by white water<sup>2</sup> and a recirculation flow from the deculator. More filler is added to the stock just after the white water tank. The first cleaning process is a five stage hydrocyclone arrangement, mainly intended to separate heavy particles from the flow. The accept from the first stage of the hydrocyclones goes to the deculator where air is separated from the stock. The second cleaning process is two parallel screens, which separates larger particles from the stock. Retention aid is added to the stock at the outlet of the machine screens. The retention aid is a cationic polymer which, amongst others, adsorb onto anionic fibers and filler particles and cause them to flocculate. The flocculation mechanism is the key for retaining small fiber fragments (fines) and filler particles on the wire. Non-flocculated filler particles will in general be too small to be retained on the wire, although mechanical entrapment of particles can be a significant mechanism (Bown 1996). In the headbox the pulp is distributed evenly onto the fine mesh, woven wire cloth. Most of the water in the pulp is recirculated to the white water tank, while a share of fiber material and filler particles form a network on the wire which will soon become the paper sheet. The pulp flow from the white water tank, through the hydrocyclones, deculator, screens, headbox, onto the wire and back to the white water tank is denoted the “short circulation”.

In the wire section, most of the water is removed by draining. In the press section, the paper sheet is pressed between rotating steel rolls, thus making use of mechanical forces for water removal. Finally, in the dryer section the paper sheet passes over rotating and heated cast iron cylinders, and most of the water left in the sheet is removed by evaporation. The paper is then accumulated on the reel before it is moved on to further processing.

### 3 The Full Scale Model

A black-box overview of the system is given in Figure 2. The manipulated inputs to the system are the amount of thick stock ( $u_t$ ), the amount of filler added to the short circulation ( $u_c$ ), and the amount of retention aid ( $u_r$ ). The outputs from the system are the basis weight ( $y_w$ ), the paper ash content ( $y_a$ ), and the white water total consistency ( $y_c$ ). The basis weight and the paper ash content are measured between the dryer section and the reel, while the white water total consistency is measured in the flow from the wire to the white water tank. The paper ash content is the amount of filler in the paper (the weight of the ash from a burned piece of paper approximately equals the weight of filler in the paper).

The model is basically covering those elements (chests, tanks, pipes, etc.) found in Figure 1. Typically, there are mass-balances of (longer) fiber, fiber fines, and the

---

<sup>2</sup>White water is the drainage from the wire. It is stored in the white water tank.

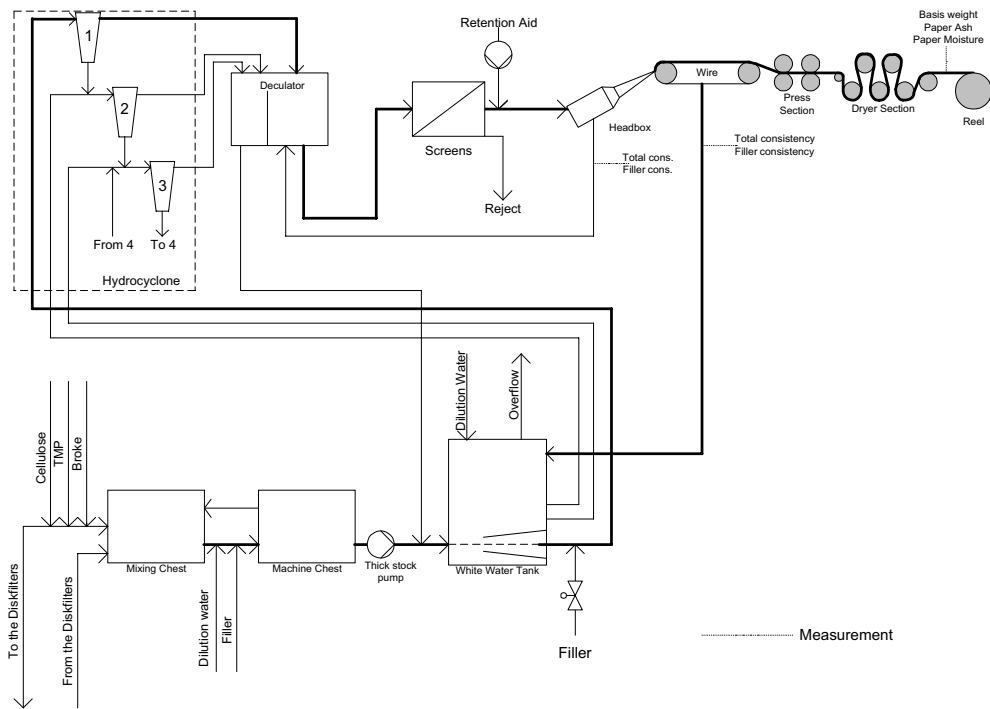


Figure 1: An overview of the paper machine.

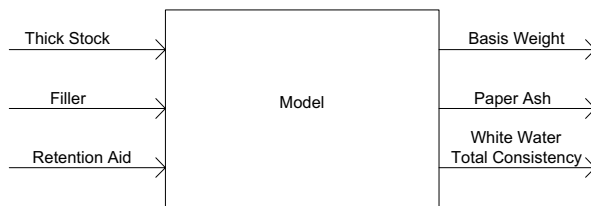


Figure 2: Inputs and outputs from the model.

two filler types for every significant volume, i.e.

$$\frac{dm_i}{dt} = \sum_j w_{i,j}, \quad (1)$$

where  $m_i$  is mass of component  $i$  in some volume, and  $w_{i,j}$  is mass flow  $j$  of component  $i$  into this volume. In the short circulation there are also mass-balances for flocculated components and retention aid. Most pipelines are modeled by partial differential equations (time delays), i.e.

$$\frac{\partial C_i}{\partial t} = -v \cdot \frac{\partial C_i}{\partial x}, \quad (2)$$

where  $C_i$  is the concentration of component  $i$ , and  $v$  is the velocity of mass flow in the pipeline. The addition of retention aid causes fibers and fillers to flocculate. The flocculation takes place in the short circulation, and is here modeled by second order kinetic equations like

$$\frac{\partial C_{floc,i}}{\partial t} = -v \cdot \frac{\partial C_{floc,i}}{\partial x} + \frac{k_i}{\rho} \cdot C_i \cdot C_{ret.aid}, \quad (3)$$

where  $C_{floc,i}$  is the concentration of flocculated mass of component  $i$ ,  $C_i$  is the concentration of component  $i$  (non-flocculated),  $k_i$  is a flocculation constant,  $\rho$  is the density of the mass flow, and  $C_{ret.aid}$  is the concentration of retention aid. Elements like the screens, headbox and wire are basically modeled with static/algebraic equations, considering the relatively small volumes involved.

The number of ordinary differential equations (ODE) is 34, and there are 104 partial differential equations (PDE). The PDE's are discretized in x-direction, bringing the total number of ODE's to 554. In this paper we omit the model for the thick stock, thus the system to study is between the thick stock pump and the reel. The reason for this being that new measurements for total consistency and ash consistency in the thick stock will be installed at PM6, thus making the thick stock model superfluous. The number of ODE's and PDE's are down to respectively 28 and 100, making the total number of ODE's (after discretization) 528.

## 4 Complexity Reduction

### 4.1 Input signals

Filtered PRBS's (Pseudo Random Binary Signals) are used as test and identification inputs to the system, and are shown in Figure 3. This type of input is widely used in identification experiments for linear systems/models (Ljung 1999) (Söderström & Stoica 1989).

The data are collected in the neighborhood of a typical operating condition of the paper machine. The most important variables defining this operating condition are given in Table 1.

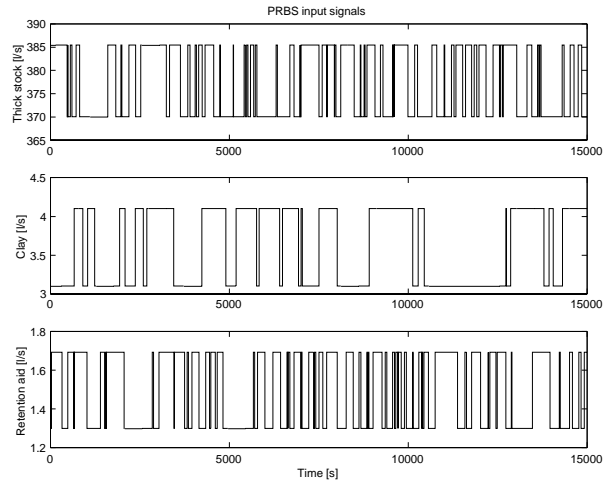


Figure 3: The filtered PRBS input signals used for identification and model reduction.

Table 1: Variable values describing the operating condition for identification.

Thick stock, flow	3701/s
Thick stock, total consistency	3.72%
Thick stock, filler consistency	1.47%
Addition of filler to the short circulation	3.11/s
Addition of retention aid to the short circulation	1.31/s
Basis weight	49.2 g/m <sup>2</sup>
Paper ash content	29.9%
Wire tray, total consistency	0.78%
Wire tray, ash consistency	0.61%
Headbox, total consistency	1.47%
Headbox, ash consistency	0.83%
Machine velocity	1500 m/min

Table 2: Sum of squared errors for mechanistic models.

Order	38 <sup>3</sup>	38	87	161
$SSE_w$	40	89	18.5	5.4
$SSE_a$	10.8	28	2.7	1.2
$SSE_c$	0.011	0.025	0.03	$8.5 \cdot 10^{-4}$

## 4.2 Measuring the error

The test signals are the filtered PRBS signals of Figure 3, and the calculated sum of squared errors (SSE)

$$SSE_i = \sum_{k=1}^N (\hat{y}_{i,k} - y_{i,k})^2, \quad (4)$$

is used as a measure of the error introduced by the simplifications. Here,  $\hat{y}_i$  is the simulated  $i^{th}$  output from the reduced order model,  $y_i$  is the simulated  $i^{th}$  output from the full scale model, and  $N$  is the number of samples. The  $i$ 's in the SSE's are denoted as  $w$  (basis weight),  $a$  (paper ash content) or  $c$  (wiretray concentration). The predictions  $\hat{y}_i$  are centered so that they have the same mean value as the full scale model responses  $y_i$ , before the SSE's are calculated.

In this paper we only consider horizons in which only the initial values are known. This is often written as  $\hat{y}_{k|0}$ , i.e. the predicted output  $\hat{y}$  at time  $k$ , given  $y$  at time 0. Another well known predictor is the one-step-ahead predictor  $\hat{y}_{k+1|k}$ .

## 4.3 Reduced mechanistic models

The full scale model is based on physical and chemical laws and balances. In this section we use our physical knowledge about the process, along with common sense, to reduce the complexity and size of the model.

In Figure 4 the full scale model responses are shown along with a 38<sup>th</sup> order model. Based on the observed sum of squared errors (SSE) for various reduced models, it is chosen to concentrate on a 38<sup>th</sup> order model, an 87<sup>th</sup> order model and a 161<sup>th</sup> order model for the comparison with other models. For the 38<sup>th</sup> order model it is also chosen to optimize the behavior by tuning some key parameters in the model. These parameters are the volumes in the deculator, and in a reject tank between the fourth and fifth stage of the hydrocyclones, and the clay and fines flocculation constants. The physical insight of the model is only negligibly degraded by the optimization, although e.g. the optimized volumes no longer have the correct physical value. The sum of squared errors (SSE) are given in Table 2.

The reduction in computation time from the 161<sup>th</sup> order model to the 38<sup>th</sup> order model was approximately 50%, while the reduction from the full scale model to the 38<sup>th</sup> order model was more than 80%.

---

<sup>3</sup>Optimized.



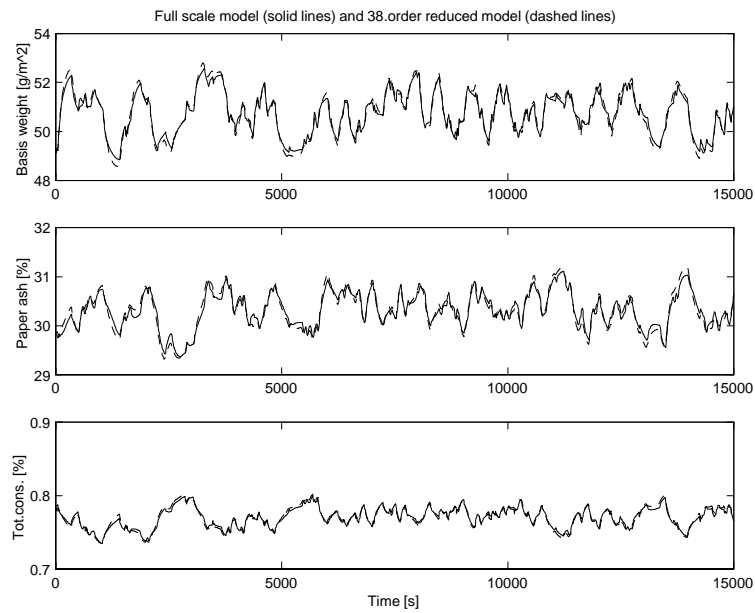


Figure 4: The responses of the full scale model (solid lines) and of a 38<sup>th</sup> order reduced mechanistic model (dashed lines). The PRBS input signals are shown in Figure 3.

### 4.3.1 The simplifications

In a model reduction effort it is natural to look at the discretization of the PDE's. In the full scale model each pipeline is discretized into 5 volumes making the pipeline delays the largest contributor to the number of states in the model. Simulation showed that by replacing every PDE outside of the main flow (thick line in Figure 1) by one ODE, the model behavior was essentially the same. This immediately reduced the number of states from 528 to 256. In addition the pipelines between the machine chest and white water tank and between the white water tank and the first stage of the hydrocyclones could also be discretized into one volume without affecting the model behavior too much. These simplifications combined with several lumped volumes in the hydrocyclones, and the inclusion of the volume of the pipeline between the deculator (left side) and the white water tank into the deculator (left side) gave the 161<sup>th</sup> order reduced model.

The 87<sup>th</sup> order model is the result of a continuation of reductions and simplifications on the 161<sup>th</sup> order model:

- The pipeline between the deculator (right side) and the screens are discretized into one volume
- The wire-, press- and dryer sections are discretized into one “volume”
- Several pipeline volumes in the hydrocyclone arrangement are included in a reject tank between the fourth and fifth stage
- Several pipeline volumes are included in the deculator:
  - The pipeline volume between the headbox and the deculator
  - The pipeline volume between the machine chest and the white water tank
  - The pipeline volume between the hydrocyclones first stage and second stage pump
  - The pipeline volume between the hydrocyclones second stage pump and the second stage
  - The pipeline volume between the hydrocyclones second stage and third stage pump
  - The pipeline volume between the hydrocyclones third stage pump and third stage
  - The pipeline volume between the hydrocyclones fourth stage and third stage pump.

The 38<sup>th</sup> order model results from a continuation of reductions and simplifications on the 87<sup>th</sup> order model:

- The pipeline volume between the deculator (right side) and the screens, is included in the deculator

- The pipeline volume between the white water tank and the first stage of the hydrocyclones, is included in the deculator
- The pipeline between the screens and the headbox is discretized into one volume.

#### 4.4 Reduced empiric (black-box) models

In this section, several black-box identification schemes will be used to identify “simple” linear models. Input-output data from the full scale model are collected, and models will be identified by prediction error and subspace methods. The data are collected in the neighborhood of a typical operating condition of the paper machine. The most important variables defining this operating condition are given in Table 1.

##### 4.4.1 Transfer matrix models

The responses of the process to step inputs are saved on file. In turn, the data from one input and one output are used to fit the parameters in a first- and second-order model (transfer function) with time delay:

$$y(s) = \frac{K}{\tau_1 s + 1} e^{-\tau_3 s} \cdot u(s) \quad (5)$$

$$y(s) = \frac{K}{(\tau_1 s + 1) \cdot (\tau_2 s + 1)} e^{-\tau_3 s} \cdot u(s) \quad (6)$$

The time delays are found visually, while the process gains and time constants are found by applying

$$K = \frac{\lim_{k \rightarrow \infty} y_k - y_{k=0}}{U} \quad (\text{process gain}) \quad (7)$$

$$\hat{\tau}_1 = \arg \min_{\tau_1} \sum_k e_k^2 \quad (\text{time constant, first-order model})$$

$$[\hat{\tau}_1, \hat{\tau}_2] = \arg \min_{[\tau_1, \tau_2]} \sum_k e_k^2 \quad (\text{time constants, second-order model}) \quad (8)$$

where  $y_{k=0}$  is the initial output value,  $U$  is the step input size, and  $e_k$  is the error between the simulated model output and the output on file, at time  $k$ .

A first-order model is preferred whenever the fit of the second-order model is only negligibly<sup>4</sup> better. The transfer matrix is found to be:

$$\begin{bmatrix} y_w \\ y_a \\ y_c \end{bmatrix} = \begin{bmatrix} \frac{0.1020}{(169s+1)} e^{-50s} & \frac{0.5583}{(1831s+1)(617s+1)} e^{-50s} & \frac{2.7726}{32^2 s^2 + 2 \cdot 0.5 \cdot 32s + 1} e^{-12s} \\ \frac{-0.0221}{31^2 s^2 + 2 \cdot 0.5 \cdot 31s + 1} e^{-35s} & \frac{0.7051}{(1867s+1)(549s+1)} e^{-40s} & \frac{1.6916}{119^2 s^2 + 2 \cdot 0.37 \cdot 119s + 1} e^{-12s} \\ \frac{0.0013}{(203s+1)} e^{-20s} & \frac{0.020}{(1826s+1)(623s+1)} e^{-20s} & \frac{-0.1455}{(301s+1)} e^{-7s} \end{bmatrix} \cdot \begin{bmatrix} u_t \\ u_c \\ u_r \end{bmatrix} \quad (9)$$

<sup>4</sup>That is, when the difference in SSE (sum of squares) is zero for a rounded three digit number.

Table 3: Sum of squared errors for N4SID models.

Order	7	28
$SSE_w$	19.69	9.78
$SSE_a$	24.15	11.64
$SSE_c$	0.0126	0.0054

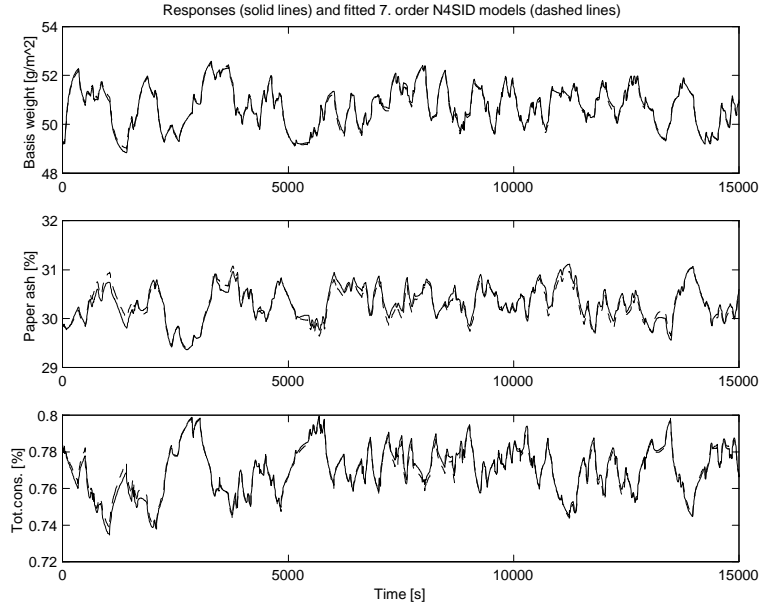


Figure 5: The responses of the full scale model (solid lines) and of a fitted 7<sup>th</sup> order N4SID model (dashed lines). The PRBS input signals are shown in Figure 3.

#### 4.4.2 N4SID subspace method

The “Numerical algorithms for Subspace State Space System Identification” method (N4SID) belongs to the subspace system identification family (Van Overschee & De Moor 1996). The method is an integrated part of the system identification toolbox (Ljung 1997) in Matlab. The data are pretreated by centering and scaling before entered into the N4SID function.

The input signals are shown in Figure 3. In Figure 5 the responses are shown along with a fitted 7<sup>th</sup> order model. Based on the observed sum of squared errors (SSE) for various model orders, it is chosen to concentrate on the 7<sup>th</sup> order model and a 28<sup>th</sup> order model for the comparison with other models. The sum of squared errors, SSE (see Equation 4), are given in Table 3.

Table 4: Sum of squared errors for DSR models.

Order	3	7
$SSE_w$	46.19	16.98
$SSE_a$	28.13	20.81
$SSE_c$	0.0211	0.0156

#### 4.4.3 DSR subspace method

The “combined Deterministic and Stochastic system identification and Realization” method (DSR) belongs to the subspace system identification family (Di Ruscio 1997). The method and software (Di Ruscio 1996) are easy to use, requiring only the data and an additional parameter to be specified. A singular value plot is supplied for helping to determine the model order. When the model order is specified, the program returns a state-space model (including the Kalman filter gain matrix, and the innovations covariance matrix) along with the initial conditions. The data are pretreated by centering and scaling before entered into the DSR program.

The input signals are shown in Figure 3. In Figure 6 the responses are shown along with a fitted 7<sup>th</sup> order model. It is chosen to concentrate on a third order model and a 7<sup>th</sup> order model for the comparison with other models. The sum of squared errors, SSE (see Equation 4), are shown in Table 4.

#### 4.4.4 Prediction error method (PEM)

The celebrated prediction error method (Ljung 1999) (Söderström & Stoica 1989) is an integrated part of Matlab’s System Identification toolbox (Ljung 1997). It offers a vast amount of possibilities regarding linear model structures, such as ARMAX, BJ, FIR and state-space models. However, for MIMO (multi-input multi-output) systems, the ARMAX-type of models get complicated and they are perhaps not very suitable for such systems. The state-space model, is however often preferred for representation of MIMO systems.

Unlike the subspace methods, the PEM is an iterative method, based on minimization of the prediction error. The fact that it is iterative limits the possible number of free parameters in the model structure dramatically, and one should not expect to be able to identify high order models (even when one is using a canonical form). A recommended method (Ljung 1997) for identifying MIMO models is to use a subspace method (such as N4SID or DSR) to identify an initial model, and use the parameters of this model as initial values for the PEM method. This approach is taken here, although the 7<sup>th</sup> and 28<sup>th</sup> order models were not improved by the PEM method, probably due to too many free parameters involved. The third order DSR model were improved by the PEM method, and the sum of squares (see Equation 4) are as given in Table 5.

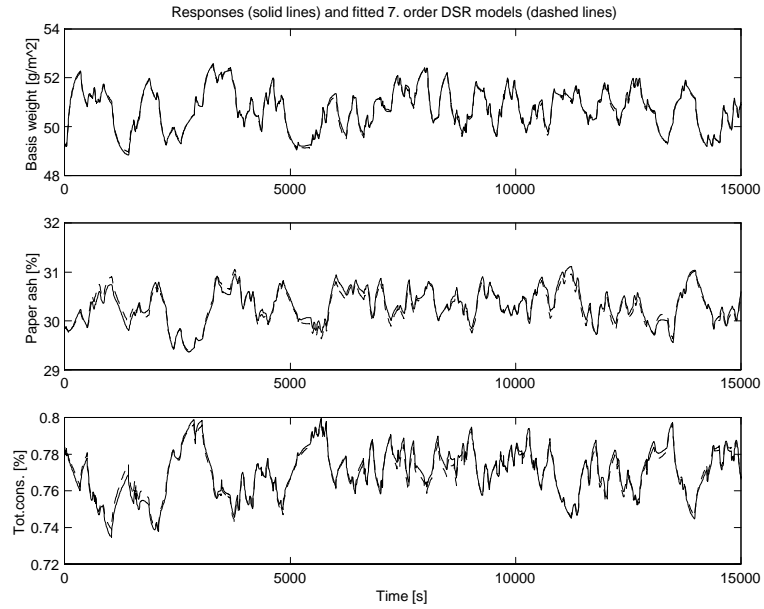


Figure 6: The responses of the full scale model (solid lines) and of a fitted  $7^{th}$  order DSR model (dashed lines). The PRBS input signals are shown in Figure 3.

Table 5: Sum of squared errors for PEM model.

Order	3
$SSE_w$	41.02
$SSE_a$	21.81
$SSE_c$	0.01716

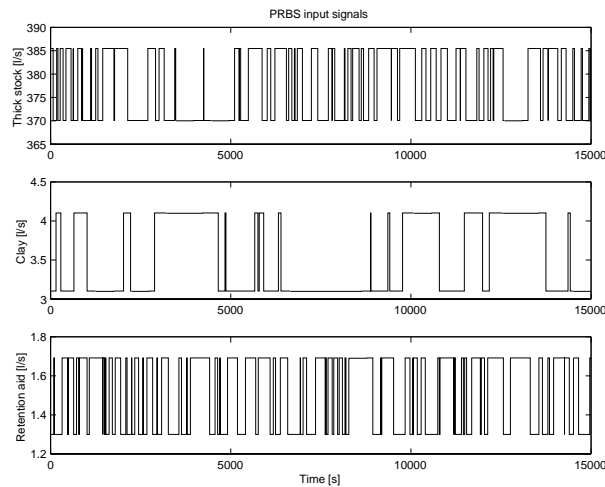


Figure 7: The filtered PRBS signals used for validation of the models. The overall operating condition of the paper machine is the same as when the models were identified.

## 5 Comparison of the Models: Prediction Ability

### 5.1 Prediction of future outputs without change in operating condition

New input signals are designed and applied to the full scale model. The levels of the input signals are such that the overall operating condition of the paper machine is in the neighborhood of that given by the variables in Table 1. The new input signals are shown in Figure 7.

The SSE's (see Equation 4) for the empirically identified and reduced mechanistic models are given in Table 6.

The PEM, DSR and N4SID models have good prediction ability, although the SSE's have increased significantly as compared to the identification. The SSE's of the mechanistic models are in some cases lower (better), and in some cases higher than in Chapter 4.3.

### 5.2 Prediction of future outputs with change in operating condition

Yet another set of input signals are designed, differing from previously used signals such that the overall operating condition of the paper machine is changed. The most

---

<sup>5</sup>Time delays are not included.

<sup>6</sup>Optimized.

Table 6: Sum of squared errors for reduced and identified models. The operating condition is comparable to that at the time of identification.

Method	Order	$SSE_w$	$SSE_a$	$SSE_c$
TM*	15 <sup>5</sup>	266	76	0.046
PEM	3	76	32	0.036
DSR	3	82	46	0.043
DSR	7	47	29	0.041
N4SID	7	55	32	0.034
N4SID	28	36	12	0.018
Mech. <sup>6</sup>	38	41	11	0.011
Mech.	38	75	25	0.021
Mech.	87	18	2.2	0.003
Mech.	161	5	0.9	$8 \cdot 10^{-4}$

\*Transfer Matrix

Table 7: Variable values describing a new operating condition for validation.

Thick stock, flow	4361/s
Thick stock, total consistency	3.72%
Thick stock, filler consistency	1.47%
Addition of filler to the short circulation	5.951/s
Addition of retention aid to the short circulation	2.01/s
Basis weight	56 g/m <sup>2</sup>
Paper ash content	32%
Wire tray, total consistency	0.78%
Wire tray, ash consistency	0.62%
Headbox, total consistency	1.47%
Headbox, ash consistency	0.85%
Machine velocity	1650 m/min

important variables to describe this new operating condition are given in Table 7.

The input signals are shown in Figure 8, and the SSE's (see Equation 4) for the empirically identified and reduced mechanistic models are given in Table 8.

The PEM, DSR and N4SID models are identified at a different operating condition, and thus it is not a surprise that the prediction ability is decreased (except for some of the  $y_c$  outputs, for which the ability has improved). The mechanistic models are producing better predictions than previously (with a few exceptions).

Figure 9 shows the responses from the full scale model and the third order DSR predictions.

---

<sup>7</sup>Time delays are not included.

<sup>8</sup>Optimized.



Table 8: Sum of squared errors for reduced and identified models. The operating condition is different from what was used for identification.

Method	Order	$SSE_w$	$SSE_a$	$SSE_c$
TM*	15 <sup>7</sup>	275	57	0.050
PEM	3	110	60	0.035
DSR	3	148	101	0.074
DSR	7	93	63	0.032
N4SID	7	98	59	0.030
N4SID	28	74	31	0.016
Mech. <sup>8</sup>	38	40	8	0.0078
Mech.	38	43	13	0.011
Mech.	87	17	3	0.0022
Mech.	161	6.5	0.8	$8.5 \cdot 10^{-4}$

\*Transfer Matrix

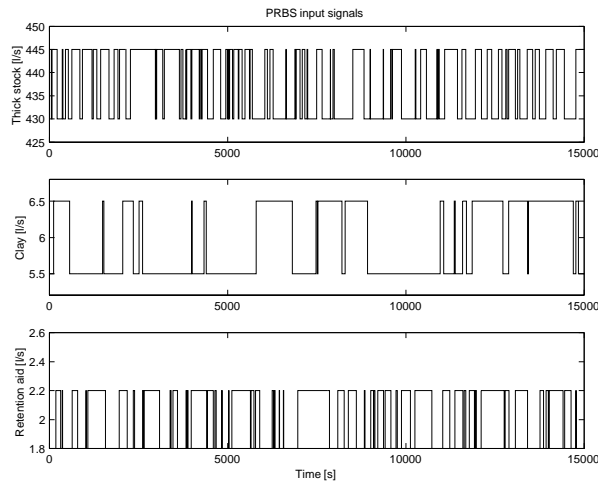


Figure 8: The filtered PRBS signals used for validation of the models. The overall operating condition of the paper machine is different from what was used for model identification and reduction.

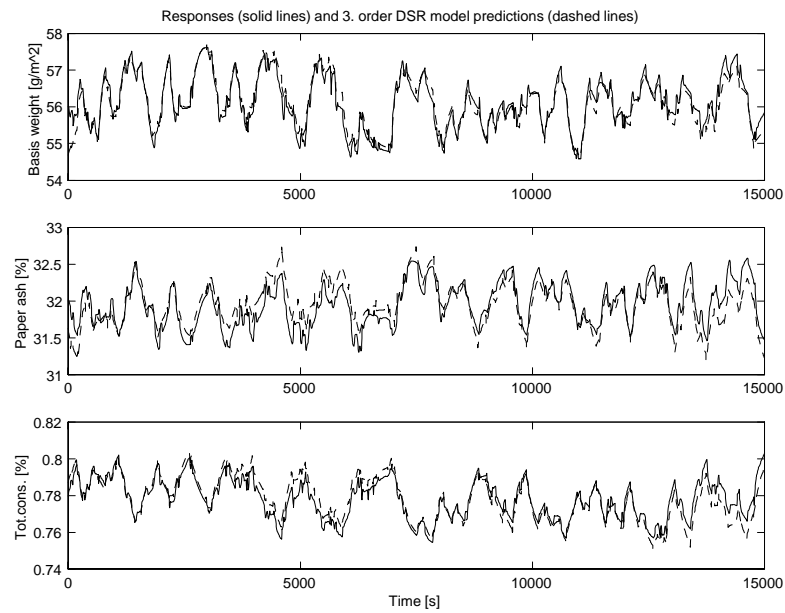


Figure 9: Full scale model responses (solid lines) and third order DSR model predictions (dashed lines), after change in operating condition.

## 6 Conclusions

The efforts made in this paper has been to study the possibilities for reducing the complexity of a paper machine model, and how the reduction affects the prediction abilities. The predictions for the various models are compared to the output from a mechanistic model of 528 ordinary differential equations (ODE). One should be aware that the full scale mechanistic model by no means represents the true system, although it is considered to do so in the comparisons of this paper.

For three different sets of input-output data, it is shown that the 528 order mechanistic model can be reduced to a 161 order mechanistic model with negligible effect. Mechanistic models using 87 and 38 ODE's are also validated with three different data sets, as are empiric models of order between 3 and 28. The mechanistic models in this paper are distinguished from the empiric models in several ways:

- The empiric models are much simpler than the mechanistic models. The empiric models usually have low order and they are linear, while the mechanistic models are of higher order and they are non-linear.
- The simulation time for the empiric models are much shorter than for the mechanistic models.
- It takes much more effort to develop a mechanistic model of a paper machine than it does to find an empiric model. However, to find a high order empiric model demands extensive experimentation on the paper machine, which is often impossible.
- The prediction ability of the empiric models strongly depends on the operating condition of the paper machine, compared to the operating condition at which the model was identified. The prediction ability at the same operating condition as in the identification, is generally very good. The prediction ability deteriorates as the operating condition is shifted away from the condition at the time of identification.
- The prediction abilities of the mechanistic models are (close to) constant, and are in most cases only negligibly affected by changes in the operating condition.

It is not possible, nor was it the intention with this paper, to conclude which model or model type is best for advanced control purposes. The various models has their specific attributes which are summarized in the list above, and it will be necessary to run tests on the real paper machine before one decides which model is best suited for the purpose.

**Acknowledgments** The authors would like to thank the employees at PM6, and especially Roger Slora, for their cooperation in providing information for this paper and for their general helpfulness. We also wish to express our thanks to associate professor Rolf Ergon for taking time to examine and pointing at errors in an earlier

version of this paper, and to associate professor David Di Ruscio and Finn Haugen for L<sup>A</sup>T<sub>E</sub>X help. The work of Tor Anders Hauge is financially supported by the Research Council of Norway (project number 134557/410) with additional financial support by Norske Skog Saugbrugs.

## References

- Andersson, L. (1997), Comparison and simplification of uncertain models, Licentiate thesis, Department of Automatic Control, Lund Institute of Technology.
- Bown, R. (1996), Physical and chemical aspects of the use of fillers in paper, *in* J. Roberts, ed., ‘Paper Chemistry’, 2 edn, Chapman and Hall.
- Di Ruscio, D. (1996), ‘DSR toolbox for MATLAB’. Copyright, Fantoft Process, Norway.
- Di Ruscio, D. (1997), A method for identification of combined deterministic stochastic systems, *in* M. Aoki & A. Havenner, eds, ‘Applications of Computer Aided Time Series Modeling’, Springer Verlag, New York.
- Diwekar, U. M. (1994), ‘How simple can it be? - a look at the models for batch distillation’, *Computers & chemical Engineering* **18**, S451–S457.
- Hauge, T. A. & Lie, B. (2000), Stabilization of the wet end at PM6. part 2: Introductory process description and modeling, A-rapport TAH20001, Norske Skog Saugbrugs, Halden, Norway (confidential and in Norwegian).
- Ljung, L. (1997), *System Identification Toolbox - For Use with Matlab*, The MathWorks, Inc.
- Ljung, L. (1999), *System Identification. Theory for the User*, 2 edn, Prentice Hall PTR.
- Norske Skog (2000), Norske Skog internet page at [www.norske-skog.com](http://www.norske-skog.com).
- Öhman, M. (1998), Trajectory-based model reduction of nonlinear systems, Licentiate thesis, Department of Automatic Control, Lund Institute of Technology.
- Slora, R. (1999), Wire tray consistency control at PM6, PM6-Rapport RSL9904, Norske Skog Saugbrugs, Halden, Norway (confidential and in Norwegian).
- Söderström, T. & Stoica, P. (1989), *System Identification*, Prentice Hall International.
- Van Overschee, P. & De Moor, B. (1996), *Subspace Identification for Linear Systems*, Kluwer Academic Publishers.